JTTEE5 19:1155–1162
DOI: 10.1007/s11666-010-9510-3
1059-9630/$19.00 © ASM International

Numerical Study on the Effect of Substrate Angle on Particle Impact Velocity and Normal Velocity Component in Cold Gas Dynamic Spraying Based on CFD

Shuo Yin, Xiao-fang Wang, Wen-ya Li, and Bao-peng Xu

(Submitted January 17, 2010; in revised form April 4, 2010)

Numerical study was conducted to investigate the effect of substrate angle on particle impact velocity and normal velocity component in cold gas dynamic spraying by using three-dimensional models based on computational fluid dynamics. It was found that the substrate angle has significant effect on particle impact velocity and normal velocity component. With increasing the substrate angle, the bow shock strength becomes increasingly weak, which results in a gradual rise in particle impact velocity. The distribution of the impact velocity presents a linearly increase along the substrate centerline due to the existence of the substrate angle and the growth rate rises gradually with increasing the substrate angle. Furthermore, the normal velocity component reduces steeply with the increase in substrate angle, which may result in a sharp decrease in deposition efficiency. In addition, the study on the influence of procedure parameters showed that gas pressure, temperature, type, and particle size also play an important role in particle acceleration.

Keywords bow shock, cold gas dynamic spray, impact velocity, numerical simulation, substrate angle, Three-dimensional model

1. Introduction

Cold gas dynamic spray (CGDS), also called cold spray, represents a radical difference from the conventional thermal spray. The deposition process relies purely on kinetic energy rather than the combination of thermal and kinetic components. In this process, spray particles are accelerated to a high velocity, ranging from 300 to 1200 m/s, by the supersonic gas flow which is generated in the convergent-divergent de Laval nozzle. Coating is formed through the intensive plastic deformation of particles at a temperature well below the melting point of spray material (Ref 1-3). The relatively low particle temperature makes the formation of oxygen-free metallic coatings to be realized, which can ensure the powder feedstock to retain the original properties. Therefore, CGDS has been drawing more and more attention due to its unique advantages.

Generally, it has been well known that there exists a material-dependent critical velocity, above which particles can adhere to the substrate and form a coating (Ref 4-8). Experimental method was always used to determine critical velocity. However, considering the economical efficiency of experiment, researchers have been trying to develop new numerical method for estimating critical velocity. Recently, a new definition that thermal boost-up zone (TBZ) was proposed to estimate the occurrence of the adiabatic shear instability and thus critical velocity, which seems relatively reasonable at present (Ref 6). Besides, the relationship between particle velocity and deposition efficiency has been widely investigated by different researchers (Ref 8-10). Previous study showed that although particle impact velocity significantly affects the deposition efficiency, the normal velocity component seems more important, playing a decisive role (Ref 10). Particles with lower normal velocity component will erode the substrate and be washed away by the gas flow. Only if the normal velocity component is sufficiently large, particles could successfully be deposited on the substrate and form a cold sprayed coating (Ref 8, 10).

Besides, there also has been growing interest to the gas flow and particle acceleration in CGDS during the past few years. The existing studies on this field mainly focused on two aspects, including the optimal design of nozzle geometry and the influence of relevant procedure parameters on gas flow and particle acceleration (Ref 11-20). Considering the economical efficiency of the experiment, most of the

This article is an invited paper selected from presentations at the 4th Asian Thermal Spray Conference (ATSC 2009) and has been expanded from the original presentation. ATSC 2009 was held at Nanyang Hotel, Xi'an Jiaotong University, Xi'an, China, October 22-24, 2009, and was chaired by Chang-Jiu Li.

Shuo Yin and **Xiao-fang Wang**, School of Energy and Power Engineering, Dalian University of Technology, Dalian 116024, Liaoning, China; **Wen-ya Li**, Shaanxi Key Laboratory of Friction Welding Technologies, Northwestern Polytechnical University, Xi' an 710072, China; and **Bao-peng Xu**, Faculty of Engineering, Kingston University, Friars Avenue, London SW15 3DW, UK. Contact e-mail: yinshuo0511@yahoo.cn.

previous researches resorted to numerical methods. And some experimental observations and measurements have confirmed that computational fluid dynamics (CFD) tools can provide accurate results of gas flow as well as particle acceleration in CGDS (Ref 16, 21-23).

As for the optimal design, Dykhuizen et al. (Ref 11) firstly proposed the optimal design of nozzle shape to obtain a high particle impact velocity based on one-dimensional isentropic assumptions. Later, Alkhimov et al. (Ref 12) provided the optimal design proposal of the nozzle geometrical dimensions according to their experimental data. Li and co-workers (Ref 13, 14) subsequently examined some geometric parameters which significantly affect the particle acceleration in the converging-barrel (CB) and converging-diverging (CD) nozzles by using a numerical method to optimize the nozzle design. Moreover, Jodoin (Ref 15) obtained the optimal exit Mach number of 1.5-3.0 through both numerical and experimental methods. Recently, Pattison et al. (Ref 16) provided the comprehensive experimental investigation on the effect of standoff distance on particle impact velocity and deposition efficiency. They found that the medium standoff region from the nozzle outlet is the optimal distance, where the bow shock has disappeared and the deposition efficiency could increase (Ref 16).

When it comes to the influence of procedure parameters, Stoltenhoff et al.'s study (Ref 17) showed the effect of inlet stagnation pressure, inlet stagnation temperature, particle diameter, and standoff distance on the gas flow and particle acceleration using a commercial software FLUENT. Some further experiments conducted by other researchers provided evidence to their numerical results (Ref 16, 18). The effect of particle size on particle acceleration was also studied in detail by Jen et al. (Ref 19) using the same software FLUENT. Meanwhile, they paid special stress on the gas flow structure inside and outside the nozzle, obtaining the insight into the flow field in CGDS (Ref 19). Moreover, Samareh and Dolatabadi (Ref 20) employed numerical method to analyze the effect of substrate shape on the gas flow structure and the particle velocity distribution by using three-dimensional model, which taken the nonplain substrate into consideration.

Notwithstanding these findings, several important problems concerning about the influence factors of particle impact velocity still need to be further studied. Under some circumstances, the substrate is probably oblique to the particle incident velocity, which may affect the gas flow and particle acceleration. Therefore, in this study, by the aid of the commercial software FLUENT, numerical simulation was conducted to examine the effect of substrate angle on particle impact velocity and normal velocity component in CGDS.

2. Numerical Methodology

2.1 Geometry

The schematic of the nozzle and the substrate used in this study is shown in Fig. 1. The nozzle has a circular cross section with the inlet diameter and outlet diameter of 10 mm and 4 mm, respectively. The convergent section has a length of 30 mm, which is attached to the throat section with a diameter of 2 mm and the following divergent section with a length of 40 mm. Particles are released from the outlet of the powder injector which is located at the position of 5 mm downstream from the nozzle inlet. The flat substrates are circle plates. The standoff distance between the substrate center and the nozzle outlet center is 16 mm. Substrate angle is defined as the include angle between the *Y*-axis and the substrate surface. In this study, the substrate angles are set as 0°, 15°, 30°, and 45°. The material of the substrate was chosen as copper.

2.2 Computational Domain

To perform the simulation, the commercially available software FLUENT was employed as the CFD solver to predict the gas flow field and particle acceleration in CGDS. Three-dimensional plane symmetry models were utilized to reduce the computational time. The symmetrical axis of the nozzle was defined as the centerline of the nozzle. The computational domain was meshed into a number of hexahedral cells with the surrounding region of the centerline refined to ensure the calculation accuracy.

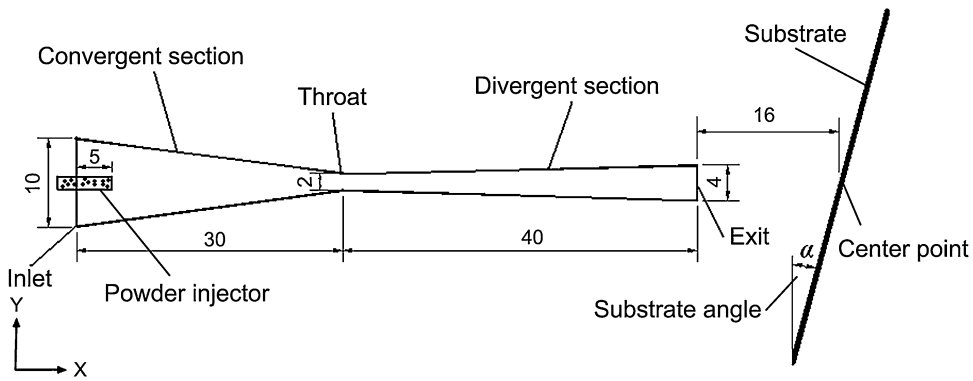

Fig. 1 Schematic of the nozzle and the substrate

The total number of the cells varies between 197,271 and 317,682, depending on the angle of the substrate. Pressure-based boundary conditions were applied to the inlet, outlet, and other atmospheric boundaries. No-slip condition was used at the nozzle wall and the substrate surface because the gas velocity near the wall zone is much low. In this study, the heat transfer process between the gas and the wall was not considered, thus a fixed heat flux of zero was enforced at the wall.

2.3 Gas Phase and Particle Phase

The gas phase was treated as continuous phase and governed by the ideal gas law which takes the compressibility effects into consideration. The governing equations for gas flow also include the continuity, momentum, and energy equations. A coupled implicit pressure-based solver with the second-order accuracy was used to simulate the gas flow field. The calculation was treated as a steady state. To account for the turbulent flow, the standard K-ε turbulence model available in FLUENT was used.

The particle phase was treated as discrete phase, and the copper material was used as the sprayed particle. The accelerating and heating of particles were computed using discrete phase modeling (DPM). The effect of particle on gas flow was not considered in this study. Models describing the dynamic behavior of in-flight particles during the two-phase flow have been well documented in the FLUENT manual (Ref 24).

3. Results and Discussion

3.1 Gas Flow and Particle Acceleration

Figure 2 shows the pressure iso-surface and velocity iso-surface of the gas flow at the inlet pressure of 2.0 MPa and the inlet temperature of 500 K using N_2 as driving gas. From the pressure iso-surface shown in Fig. 2(a), it is clearly seen a well-formed complex wave structure which are composed of oblique shock, expansion wave, and bow shock. As the supersonic flow leaves the nozzle exit, oblique shock is formed due to the overexpansion, followed by expansion waves as a result of multiple reflections at the atmosphere boundary. These alternate waves result in the fluctuation of driving gas velocity, which can be clearly observed in Fig. 2(b). Moreover, it can be found that between the nozzle exit and the substrate, there exists a well-formed bow shock located close to the substrate, which arises from the interaction between the supersonic gas flow and the substrate. The pressure in this region is well confined, which leads to a sharp increase of pressure and temperature in front of the substrate. The gas flow velocity is decelerated rapidly when the gas flow penetrates into the bow shock and approaches the substrate.

Figure 3 shows the velocity and temperature development of N_2 along the nozzle centerline. It is clear that the driving gas is mainly accelerated at the throat section and the divergent section rather than the convergent section. At the current condition, the gas can be accelerated to

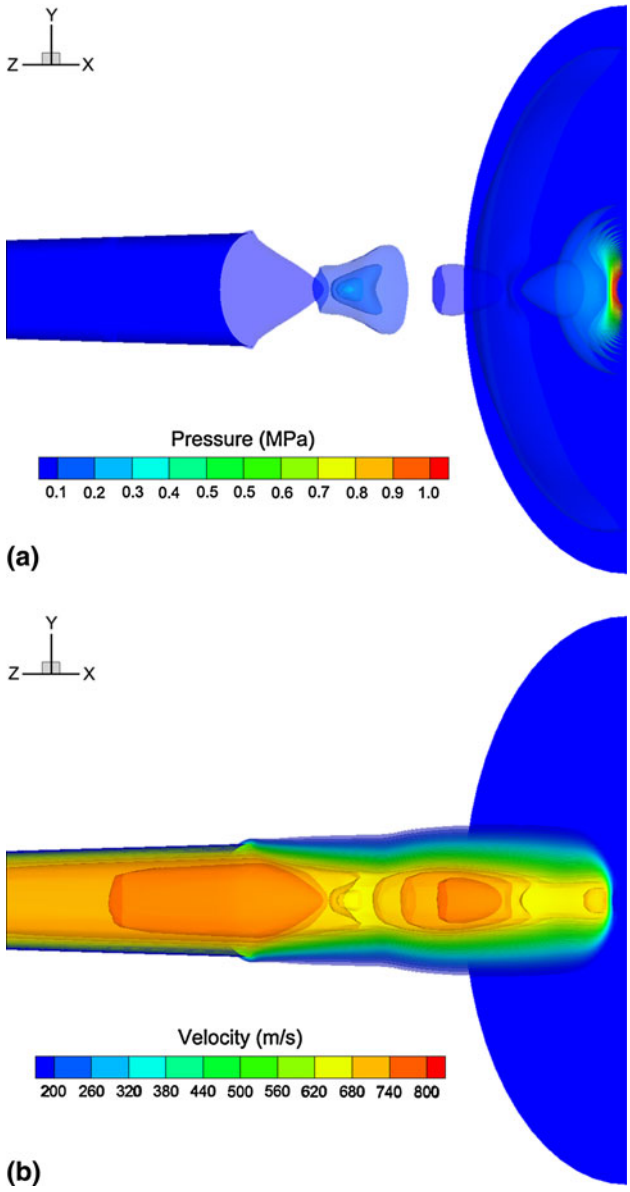

Fig. 2 Three-dimensional simulated results using N_2 as driving gas at the inlet pressure of 2.0 MPa and temperature of 500 K: (a) Pressure iso-surface. (b) Velocity iso-surface

almost 800 m/s at the nozzle exit. Moreover, at the throat section and the following divergent section, the gas velocity presents a mild fluctuation due to the cone-shape shock generated as a result of sudden expansion of the driving gas. After exiting the nozzle, the gas velocity begins to fluctuate periodically along the centerline in the form of a sharp decrease followed by a rapid increase, which arises from the oblique shock and expansion wave outside the nozzle. Then, it is decelerated sharply when penetrating into the bow shock in front of the substrate, which results in a much low impact velocity of the driving gas.

In order to obtain some features of the particle acceleration, the centerline velocity of copper particles with the diameters of 1, 10, and 20 μm are also given in Fig. 3. It is

obvious that the particle with the diameter of 1 μm can be easily driven and accelerated to a higher velocity, while the larger ones, such as the 10 μm and 20 μm particles, are accelerated difficultly. The reason for this fact can be attributed to the different masses and driven capabilities. Lower mass can achieve better-driven capability. Furthermore, it is interesting to find that the shockwaves generated inside and outside the nozzle almost have no effect on the acceleration of 10 and 20 μm copper particles. These particles are accelerated mainly through their own inertia outside the nozzle exit. Only the 1 μm particle can be slightly influenced by the oblique shock and bow shock outside the nozzle due to the smaller inertia. The fluctuation of particle velocity can be clearly observed outside the nozzle exit, which indicates the effect of the oblique shock and bow shock on particle acceleration. These results are consistent with the previous studies (Ref 10, 16, 25).

On the other hand, it is important to be pointed out that the variations of the gas and particle temperatures present an inverse tendency to the centerline velocities. The gas temperature maintains a relative high value at the convergent section and decreases steeply at the throat and divergent section. In addition, due to the low gas velocity at the convergent section, the residence time of particles is relatively long. Particles, therefore, chiefly heat up in this section and retain a higher temperature than the driving gas at the diverging section all the time. The previous one-dimensional simulation also obtained the same result as that in this study (Ref 17).

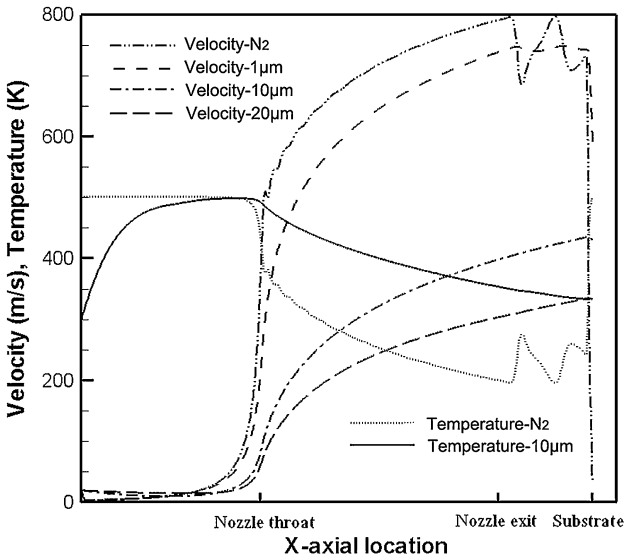

Fig. 3 Velocity and temperature development of N_2 and copper particle along the nozzle centerline

3.2 Effect of Substrate Angle on Particle Impact Velocity

Figure 4 displays the pressure iso-surface of the gas flow outside the nozzle with different substrate angles. It is clearly found that the four cases give a similar flow pattern. The oblique shock and expansion wave present periodically with the bow shock generated in front of the substrate. However, it can be noticed that the structure of the bow shock presents a great difference. The shape of the bow shock for the 0° case is regular and has been depicted in Section 3.1. However, for the 15° case, although the bow shock is also generated, its shape becomes much irregular with some oblique shock formed along the centerline of the substrate. This fact could cause the strength of the bow shock to be a little weaker than that of the 0° case. With further increasing the substrate angle, the shape of the bow shock becomes increasingly irregular and the formed oblique shock become more and more strong, thus the strength of the bow shock decreases gradually.

Figure 5 shows the effect of substrate angle on particle impact velocity under different procedure parameters. Figure 5(a) illustrates the change of particle impact velocity with the substrate angle using N_2 as driving gas under different particle sizes. It is clear that the particle impact velocity rises with increasing the substrate angle regardless of the particle size. The growth rate is much larger for small size particle, such as 1 μm particle in this simulation. This phenomenon can be attributed to the strength of the bow shock in front of the substrate. As mentioned previously, with the increscent in the substrate angle, the bow shock strength becomes increasingly weak. Thus, the effect of the bow shock on the deceleration of the particle velocity becomes weak gradually, which causes particles to achieve a relative high impact velocity when the substrate angle is larger. Moreover, it is also

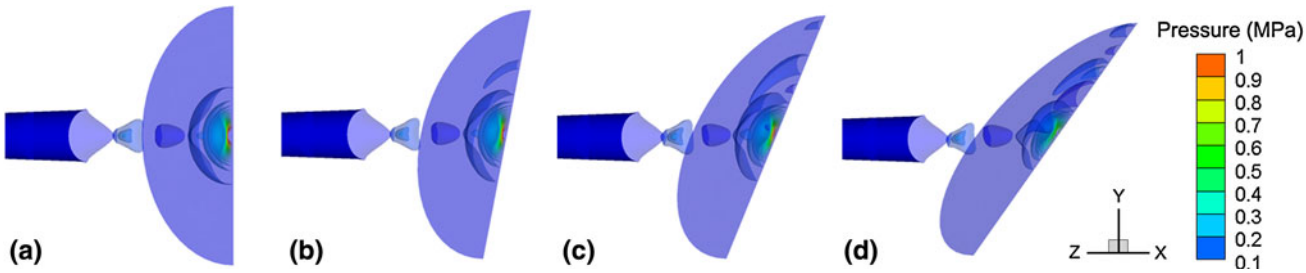

Fig. 4 Three-dimensional simulated results (pressure iso-surfaces) for different substrate angles using N_2 as driving gas at the inlet pressure of 2.0 MPa and temperature of 500 K: (a) 0°, (b) 15°, (c) 30°, and (d) 45°

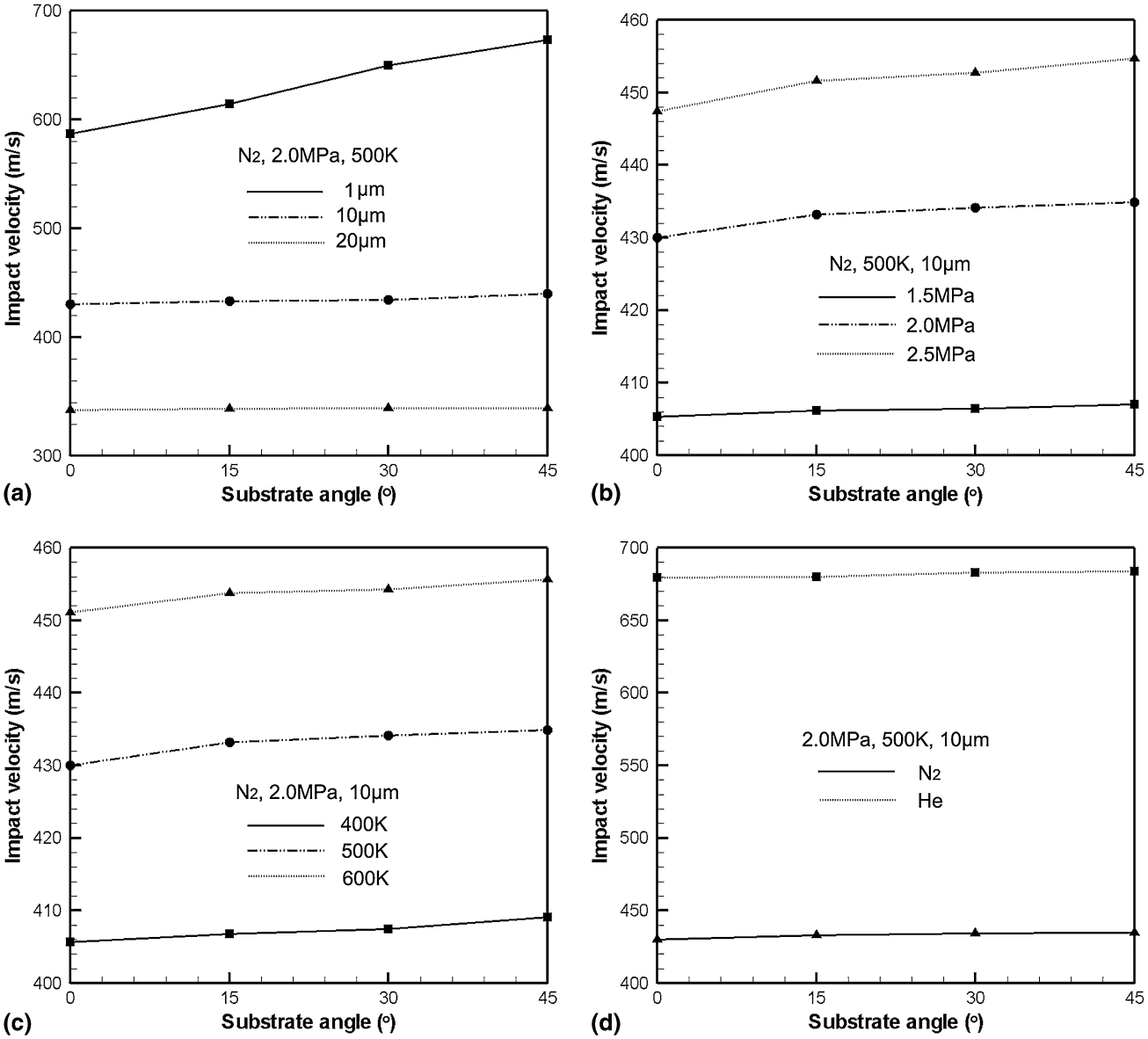

Fig. 5 Variation of particle impact velocity with the substrate angle: (a) under different particle sizes, (b) under different N_2 pressure, (c) under different N_2 temperature, and (d) under different gas types

found that the particle size has a significant effect on particle acceleration. For 1 μm particle, it is easy to be driven and accelerated to a higher value in comparison with the 10 and 20 μm particle. Nevertheless, it should be pointed out that although 1 μm particle is easy to be accelerated to a high value, taking into account the commonly used powder size distribution in CGDS (5-50 μm), it is not usually used in actual spray process.

Figure 5(b) and (c) shows the variation of particle impact velocity with the substrate angle under different pressure and temperature, respectively, using N_2 as driving gas. It is clearly seen that particle impact velocity rises with the increase in the inlet pressure as well as the temperature. Furthermore, the effect of driving gas type on particle velocity was also studied. The simulated result shown in Fig. 5(d) indicates that using He as driving gas results in a large increase in particle velocity. This is because that the sonic speed of He at the throat section which determines the particle velocity at the nozzle exit is about 2.7 times larger than that of N_2 under the same condition. These results are consistent with the experimental results in (Ref 10) and the two-dimensional numerical results in Ref 13. From Fig. 5(b-d), it also can be noticed that the particle impact velocity increases gradually with increasing the substrate angle regardless of the inlet temperature, pressure, and the gas type. This fact further proves that the substrate angle actually affects the particle impact velocity.

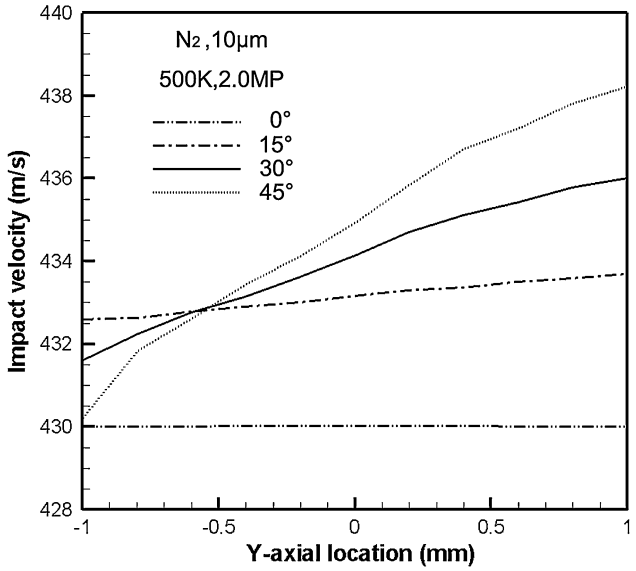

Fig. 6 Distribution of particle impact velocity along *Y*-axis

Figure 6 shows the distribution of particle impact velocity along the *Y*-axis. It is obvious that the particle impact velocities almost have a same value when the substrate is 0°. This is because that the velocity of the driving gas generally can be considered to have a same value inside the potential cone and thus the same driving capabilities. In this work, all the selected particles are inside the potential cone and hence they can achieve a same velocity when impacting the substrate. However, when increasing the substrate angle to 15°, the impact velocity presents a linearly increase along the *Y*-axis with the peak value at the location of 1 mm and the lowest value at the location of −1 mm. This fact can be attributed to the different strength of the bow shock. As mentioned above, the presence of the substrate angle results in the generation of the oblique shock along the substrate centerline, the strength of the bow shock at the direction where the oblique shock is generated should be a little weaker than the other direction. Therefore, particles can be accelerated to a higher velocity at this side. Furthermore, with further increasing the substrate angle, the discrepancy of the bow shock strength between two sides is increasingly large and thus the growth rate rises gradually. When the substrate angle is increased to 45°, the peak value and the lowest value can amount to 438 and 430 m/s, respectively.

3.3 Effect of Substrate Angle on Particle Normal Velocity Component

Gilmore et al. reported that the deposition efficiency is much dependent on the particle normal velocity component, but not the impact velocity (Ref 10). Therefore, in order to clarify the effect of substrate angle on normal velocity component and thus deposition efficiency, the variations of particle normal velocity component with the substrate angle under different procedure parameters are given in Fig. 7. It is obvious that substrate angle exerts significant influence on the normal velocity component. With increasing the substrate angle, the normal velocity component decreases steeply regardless of the particle size, temperature, pressure and type. The reason for this fact can be simply explained through the following equation:

$$v_n = v \times \cos\alpha \qquad \text{(Eq 1)}$$

where v_n is the normal velocity component, v is the impact velocity, α is the substrate angle. The values of cos 15°, cos 30°, and cos 45° are 0.966, 0.866, and 0.707, respectively. Despite the fact that the impact velocity increases with the increase in substrate angle, the product of v and cos α causes the normal velocity component much lower than the impact velocity. This lower normal velocity is so harmful to the deposition efficiency in CGDS. However, it is interesting to find that 1 μm particle achieves a higher normal velocity component while increasing the substrate angle from 0° to 15°. This is because that 1 μm particle is easy to be influenced by the driving gas. When increasing the substrate angle to 15°, the bow shock strength becomes weaker and thus particle can be accelerated to a higher velocity, but the value of cos 15° is 0.966, just 0.034 smaller than 1. Therefore, the product of 0.966 and the impact velocity cause the normal velocity component still to maintain a high value when the substrate angle reaches 15°. This phenomenon gradually disappears with further increasing the substrate angle.

4. Conclusions

Numerical investigation on the effect of substrate angle on particle impact velocity and normal velocity component was conducted by the aid of CFD tools. Owing to the nonaxisymmetrical characteristic of the calculation models, three-dimensional models were employed to reveal all features of the gas flow and particle acceleration. It has been found that particles can be accelerated to a higher velocity with smaller size, higher pressure, and temperature. Also, using He as the driving gas can achieve a higher particle velocity compared to the N_2. The substrate angle significantly affects the particle impact velocity, normal velocity component, and thus deposition efficiency. With increasing the substrate angle, the bow shock strength becomes increasingly weak, which results in a gradual rise in particle impact velocity. Besides, the substrate angle also leads to a linearly increase of the impact velocity along the substrate centerline and the growth rate rises gradually with increasing the substrate angle. In addition, the normal velocity component which is closely related to the deposition efficiency decreases sharply with the increase in substrate angle. This fact implies that the deposition efficiency may decrease when substrate is oblique to the direction of particle incident velocity.

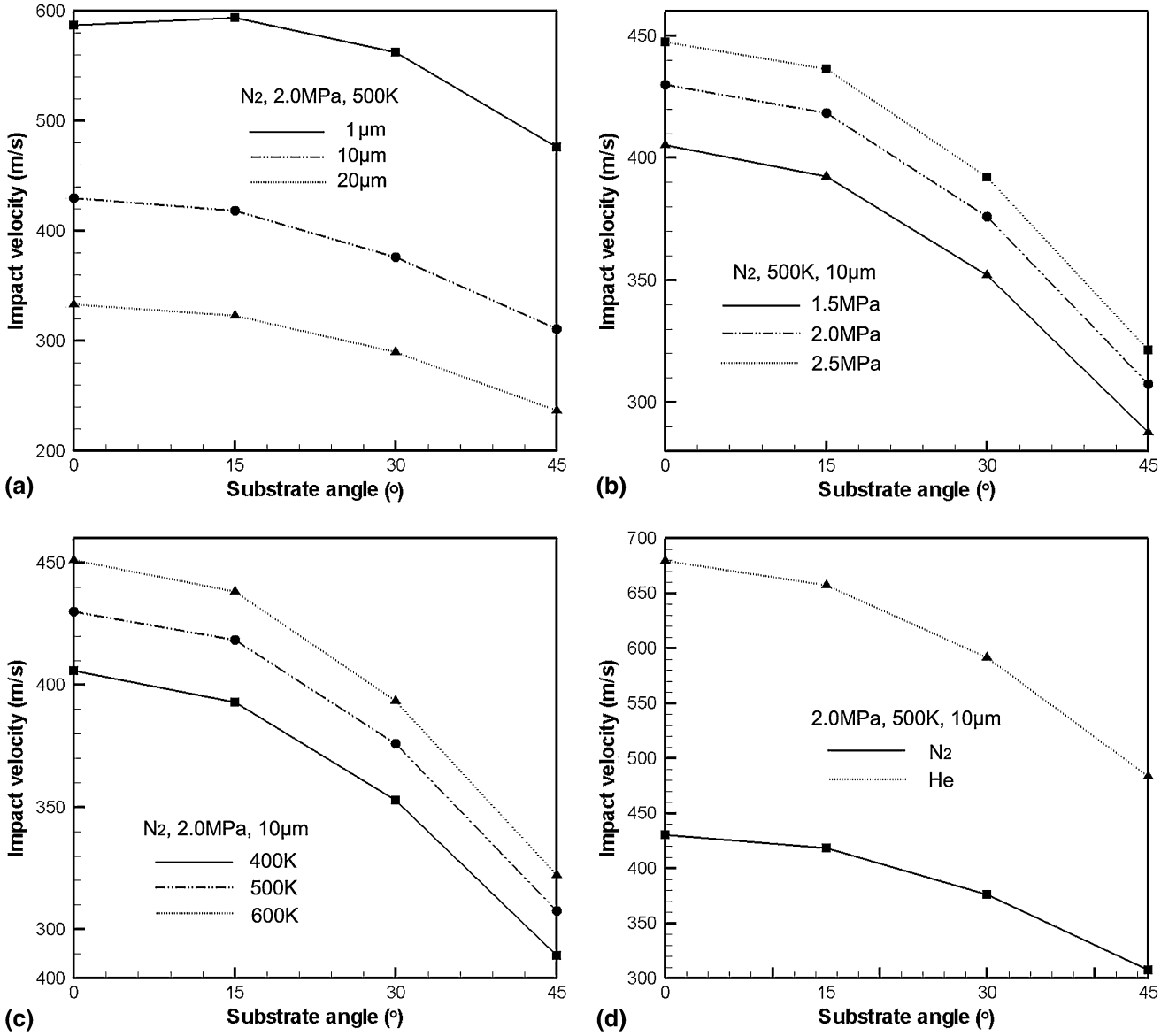

Fig. 7 Variation of particle normal velocity component with the substrate angle: (a) under different particle sizes, (b) under different N_2 pressure, (c) under different N_2 temperature, and (d) under different gas types

Acknowledgments

The authors would like to acknowledge the financial support by National 973 Basics Science Research Program (No. 2009CB724303) and the National Natural Science Foundation of China (No. 50476075).

References

1. A.P. Alkimov, V.F. Kosarev, and A.N. Papyrin, A Method of Cold Gas Dynamic Deposition, *Dokl. Akad. Nauk. SSSR*, 1990, **315**(5), p 1062-1065
2. T.H. Van Steenkiste, J.R. Smith, R.E. Teets, J.J. Moleski, D.W. Gorkiewicz, R.P. Tison, D.R. Marantz, K.A. Kowalsky, W.L. Riggs, P.H. Zajchowski, B. Pilsner, R.C. McCune, and K.J. Barnett, Kinetic Spray Coatings, *Surf. Coat. Technol.*, 1999, **111**(1), p 62-71
3. A. Papyrin, Cold Spray Technology, *Adv. Mater. Process.*, 2001, **159**(9), p 49-51
4. H. Assadi, F. Gartner, T. Stoltenhoff, and H. Kreye, Bonding Mechanism in Cold Gas Spraying, *Acta Mater.*, 2003, **51**(15), p 4379-4394
5. M. Grujicic, C.-L. Zhao, W.S. DeRosset, and D. Helfritch, Adiabatic Shear Instability Based Mechanism for Particles/Substrate Bonding in the Cold-gas Dynamic-Spray Process, *Mater. Des.*, 2004, **25**(8), p 681-688
6. G. Bae, Y. Xiong, S. Kumar, K. Kang, and C. Lee, General Aspects of Interface Bonding in Kinetic Sprayed Coatings, *Acta Mater.*, 2008, **56**(17), p 4858-4868
7. T. Schmidt, F. Gärtner, H. Assadi, and H. Kreye, Development of a Generalized Parameter Window for Cold Spray Deposition, *Acta Mater.*, 2006, **54**(3), p 729-742

8. C.-J. Li, W.-Y. Li, and H.-L. Liao, Examination of the Critical Velocity for Deposition of Particles in Cold Spraying, *J. Therm. Spray Technol.*, 2006, **15**(2), p 212-222
9. T. Schmidt, H. Assadi, F. Gärtner, H. Richter, T. Stoltenhoff, H. Kreye, and T. Klassen, From Particle Acceleration to Impact and Bonding in Cold Spraying, *J. Therm. Spray Technol.*, 2009, **18**(5-6), p 794-808
10. D.L. Gilmore, R.C. Dykhuizen, R.A. Neiser, T.J. Roemer, and M.F. Smith, Particle Velocity and Deposition Efficiency in the Cold Spray Process, *J. Therm. Spray Technol.*, 1999, **8**(4), p 576-582
11. R.C. Dykhuizen and M.F. Smith, Gas Dynamic Principles of Cold Spray, *J. Therm. Spray Technol.*, 1998, **7**(2), p 205-212
12. A.P. Alkhimov, V.F. Kosarev, and S.V. Klinkov, The Features of Cold Spray Nozzle Design, *J. Therm. Spray Technol.*, 2001, **10**(2), p 375-381
13. W.-Y. Li and C.-J. Li, Optimal Design of a Novel Cold Spray Gun Nozzle at a Limited Space, *J. Therm. Spray Technol.*, 2005, **14**(3), p 391-396
14. W.-Y. Li, H. Liao, H.-T. Wang, C.-J. Li, G. Zhang, and C. Coddet, Optimal Design of Convergent-Barrel Cold Spray Nozzle by Numerical Method, *Appl. Surf. Sci.*, 2006, **253**(2), p 708-713
15. B. Jodoin, Cold Spray Nozzle Mach Number Limitation, *J. Therm. Spray Technol.*, 2002, **11**(4), p 496-507
16. J. Pattison, S. Celotto, A. Dhan, and W. O'Neill, Standoff Distance and Bow Shock Phenomena in the Cold Spray Process, *Surf. Coat. Technol.*, 2008, **202**(8), p 1443-1454
17. T. Stoltenhoff, H. Kreye, and H.J. Richter, An Analysis of the Cold Spray Process and Its Coatings, *J. Therm. Spray Technol.*, 2002, **11**(4), p 542-555
18. S.H. Zahiri, W. Yang, and M. Jahedi, Characterization of Cold Spray Titanium Supersonic Jet, *J. Therm. Spray Technol.*, 2009, **18**(1), p 110-117
19. T.-C. Jen, L.-J. Li, W.-Z. Cui, Q.-H. Chen, and X.-M. Zhang, Numerical Investigations on Cold Gas Dynamic Spray Process with Nano- and Microsize Particles, *Int. J. Heat Mass Trans.*, 2005, **48**(21-22), p 4384-4396
20. B. Samareh and A. Dolatabadi, A Three-Dimensional Analysis of the Cold Spray Process: The Effects of Substrate Location and Shape, *J. Therm. Spray Technol.*, 2007, **16**(5-6), p 634-642
21. M. Karimi, A. Fartaj, G. Rankin, D. Vanderzwet, W. Birtch, and J. Villafuerte, Numerical Simulation of the Cold Gas Dynamic Spray Process, *J. Therm. Spray Technol.*, 2005, **15**(4), p 518-523
22. B. Samareh, O. Stier, V. Lüthen, and A. Dolatabadi, Assessment of CFD Modeling via Flow Visualization in Cold Spray Process, *J. Therm. Spray Technol.*, 2009, **18**(5-6), p 934-943
23. B. Jodoin, F. Raletz, and M. Vardelle, Cold Spray Modeling and Validation Using an Optical Diagnostic Method, *Surf. Coat. Technol.*, 2006, **10**(14-15), p 4424-4432
24. FLUENT Inc., *FLUENT 6.2 Manual*, Lebanon, NH, 1990
25. P.C. King and M. Jahedi, Relationship Between Particle Size and Deformation in the Cold Spray Process, *Appl. Surf. Sci.*, 2010, **256**(6), p 1735-1738